Anti-proliferative and anti-invasive properties of a purified fraction from *Streptomyces* sp. H7372

WAI KIEN YIP[1], SAROT CHEENPRACHA[2], LENG CHEE CHANG[2], COY CHOKE HO[3] and HENG FONG SEOW[1]

[1]Department of Pathology, Faculty of Medicine and Health Sciences, Universiti Putra Malaysia, 43400 UPM Serdang, Selangor, Malaysia; [2]Department of Pharmaceutical Sciences, College of Pharmacy, University of Hawaii Hilo, 34 Rainbow Drive, Hilo, HI 96720, USA; [3]Biotechnology Program, School of Science and Technology, Universiti Malaysia Sabah, 88999 Kota Kinabalu, Sabah, Malaysia

Received May 6, 2010; Accepted June 24, 2010

DOI: 10.3892/ijo_00000774

Abstract. Secondary metabolites from actinomycetes especially the genus Streptomyces may be one of the most important sources for novel anticancer agents. A purified fraction from a novel actinomycete strain, *Streptomyces* sp. H7372, was elucidated in breast cancer cells. We have isolated three purified fractions from a novel strain, *Streptomyces* sp. H7372. One of the fractions, designated as 31-2, exhibited the strongest growth-inhibitory effect and thereby was selected for further studies. 31-2 exerted a growth-inhibitory effect on a panel of 15 human cancer and 2 non-malignant cell lines. In MCF-7 and MDA-MB-231 breast cancer cells, 31-2 induced a cytostatic (anti-proliferative) effect without causing cytotoxicity (cell death). Our data suggest that the cytostasis resulted from cell cycle arrest at the G1 phase in MCF-7 cells and at the S phase in MDA-MB-231 cells. Western blot analysis demonstrated a modulation of phosphorylation of the Rb and CDC2 proteins and of CDK4, cyclin D1 and cyclin D3 in the 31-2-treated breast cancer cell lines. The protein levels of CDK2, CDK6, and PCNA were not affected by 31-2 treatment. 31-2 also exhibited an anti-invasive effect in MDA-MB-231 cells. However, this effect is not attributed to the modulation of proteolytic activity in MDA-MB-231 cells as the enzymatic degradation of type IV collagen was not affected by 31-2. The 31-2 is a potent cytostatic and anti-invasive agent and modulates the cell cycle pathway. Together, these results will have important implications in searching for novel approaches to treat cancer.

Introduction

Cancer chemotherapy has gradually improved with the development of newer generation cytotoxic agents such as the taxanes and gemcitabine, with curative activity against different forms of malignancy. While treatment of certain malignancies with chemotherapy has been successful and encouraging, the effectiveness has often been limited by drug resistance of tumours and by side effects on normal tissues and cells. Chemotherapy with cytotoxic agents that target proliferating neoplastic cells have very little or lack specificity resulting in undesirable adverse drug effects such as gastrointestinal, neurologic, cardiovascular, and skin toxicities, myelosuppression and hypersensitivity reactions (1). Ideal anticancer drugs would eradicate cancer cells without harming normal tissues, while evading drug resistance. With no currently available agents meeting these criteria, the continued elucidation of new biochemical mechanisms underlying drug efficacy and the search for novel agents or therapeutic strategies remain a necessity.

Microorganisms have been reported to produce around 23,000 bioactive secondary metabolites and over 45% of these compounds are discovered from actinomycetes (2). Members of the genus *Streptomyces* in this group have been well known during the last seventy years as prolific producers of new bioactive compounds, many of which are potent antibiotics and antitumour drugs (3). Clinically useful antitumour drugs produced by streptomycetes include anthracyclines (aclarubicin, daunomycin and doxorubicin), peptides (bleomycin and actinomycin D), aureolic acids (mithramycin), enediynes (neocarzinostatin), antimetabolites (pentostatin), carzinophilin, mitomycins and others (4,5). Actinomycetes have attracted great attention since they have developed unique metabolic and physiological capabilities that not only ensure survival in complex environments, but also offer the potential to produce compounds with antitumour and other interesting pharmacological activities. Efforts have been made towards novel drug discovery from soil actinomycetes inhabiting in the Sabah rain forests which house a diverse assemblage of microbes. Among the isolated actinomycete strains, *Streptomyces* sp. H7372 was indentified to inhibit Ras-Raf interaction by the yeast two-hybrid screening system (6,7). Ras and Raf play a central role in the growth factor signaling pathways controlling cell proliferation, survival, and differentiation (8,9).

Our preliminary studies have shown that the crude extract of H7372 exerts growth-inhibitory effects on human breast

Correspondence to: Professor Heng Fong Seow, Department of Pathology, Faculty of Medicine and Health Sciences, Universiti Putra Malaysia, 43400 UPM Serdang, Selangor, Malaysia
E-mail: shf@medic.upm.edu.my

Key words: Streptomyces, cytostasis, cell cycle, invasion, proteolytic activity, breast cancer

cancer cell lines. It is not surprising that the bioactive secondary metabolites produced by H7372 strain are potential sources of novel anticancer agents. Identification and isolation of bioactive compounds from H7372 strain are currently in progress by a research group based in the University of Hawaii. Several bioactive fractions, as identified from the yeast two-hybrid screening system, have been purified from H7372 crude extracts. In the present study, we elucidated the growth-inhibitory effects of three active fractions, designated as H7372-28, -31-1, and -31-2. One fraction with the most potent activity, H7372-31-2 was selected for further elucidations of its cellular and molecular mechanisms of action in two breast cancer cell lines, MCF-7 and MDA-MB-231 cells representing the estrogen receptor-positive (ER^+), progesterone receptor-positive (PR^+) and ER^-PR^- breast cancers, respectively.

Materials and methods

Cell lines. TW01, TW04, TW06, SUNE-1, and CNE-1 cell lines were generously provided by Sam Choon Kook (University Malaya, Malaysia) and Chin-Tarng Lin (National Taiwan University, Taiwan). MDA-MB-231, MCF-7, T-47D, HT-29, Caco-2, HCT116, HepG2, PC-3, DU145, HeLa, and IMR-90 cell lines were obtained from the American Type Culture Collection (Manassas, VA). LX-2 cell line was a kind gift from Scott Friedman (Mount Sinai School of Medicine, New York). All cell lines were grown in RPMI-1640 medium containing 10% fetal bovine serum (FBS) (Invitrogen Corp., Carlsbad, CA).

Extraction and fractionation. *Streptomyces* sp. H7372 was cultured in the medium containing 20 g/l D-mannitol, 20 g/l peptone, and 10 g/l dextrose (pH 7.0) at 30˚C with agitation at 250 rpm for seven days. The fermented culture broth was centrifuged and the supernatant was extracted with *n*-butanol. The organic extract was suspended in H_2O (1:1) and then partitioned successively with chloroform and ethyl acetate. The chloroform and ethyl acetate extracts were subjected to fractionation. Column chromatography (CC) was carried out using Merck silica gel 60 (70-230 mesh). Reverse-phase HPLC was carried out on the Beckman Coulter Gold-168 system equipped with a photodiode array detector using Alltech semipreparative Econosil C18 column (10 μm, 10x250 mm) and run at a flow rate at 2.0 ml/min. A fraction was isolated from the chloroform extract by CC eluting successively with hexanes and increasing polarity with acetone and methanol. The fraction was recrystallized with methanol-chloroform (1:1) to give purified fraction H7372-28 and the mother liquor was further separated by CC eluting with methanol-chloroform (1:99) and subsequently by reverse-phase HPLC with methanol-H_2O (3:1) to give purified fraction H7372-31-1 (retention time of 14.5 min). A purified fraction designated as H7372-31-2 was recrystallized from a fraction isolated from the ethyl acetate extract by CC eluting sequentially with hexanes and increasing polarity with ethyl acetate and methanol. Stock solutions of the H7372-28, -31-1, and -31-2 fractions were prepared in methanol at 10 mg/ml. Following reconstitution, all stock solutions were stored at -20˚C. The final concentrations of methanol used were <0.2% in cell culture medium. Solvent controls with equivalent concentration were included in all experiments.

Cell viability assay. MTT [3-(4,5-dimethylthiazol-2-yl)-2,5-diphenyl-2H-tetrazolium bromide] assay was used to evaluate the growth-inhibitory effects of purified fractions. The cells were seeded on 96-well plates at a density of 3,000 cells per well, incubated for 24 h, and then treated with increasing concentrations of the fractions (in 100 μl of medium/well) at 37˚C. After 72 h of treatment, 10 μl of MTT solution (5 mg/ml) (Amresco, Solon, OH) was added into each well and incubated for 3 h at 37˚C before the removal of the media. DMSO (150 μl/well) was then added to dissolve the formazan product. The absorbance at 570 nm wavelength, which is directly proportional to the number of living cells in culture, was measured using a spectrophotometric microtiter plate reader. All treatments or controls were done in triplicate wells.

Cell proliferation assay. The MCF-7 and MDA-MB-231 cells were plated in the 96-well plates at a density of 6,000 cells per well, incubated for 24 h, and then treated with 0.2 and 2 μg/ml H7372-31-2 (in 100 μl of medium/well) at 37˚C. For 0 hour and every 12 h of treatment, up to 72 h, 20 μl of the CellTiter 96® AQueous One Solution Reagent (Promega Corp., Madison, WI) was added into each well. After incubation for 3 h at 37˚C, the quantity of soluble formazan product of MTS tetrazolium was measured by the microtiter plate reader at 490 nm. Relative cell proliferation was calculated by dividing the absorbance, which is directly proportional to the cell viability, for a given time-point by the absorbance from the initial reading (hour 0) of assay. All treatments or controls were done in triplicate wells and three independent experiments were conducted.

Apoptosis assay. Apoptosis was assayed using the Annexin V-FITC Apoptosis Detection Kit (BD Biosciences, San Jose, CA). H7372-31-2-treated or control MCF-7 and MDA-MB-231 cells were collected from 6-well plates (60-80% confluency), washed with cold phosphate-buffered saline with 0.1% bovine serum albumin (PBS/BSA), and then subjected to Annexin V-FITC and propidium iodide (PI) staining following the manufacturer's instructions. The stained cells were analyzed by flow cytometry (FACSCalibur™ instrument equipped with CellQuest software; BD Biosciences). Approximately 10,000 cells were acquired and percentages of apoptotic and necrotic cells were determined by FCS Express Version 3 (De Novo Software, Los Angeles, CA). Cells treated with 2 μM staurosporine (Calbiochem®; Merck KGaA) for 5 h were used as positive control. Three independent experiments were conducted. The differences of mean values between treated and control samples were tested by One-way analysis of variance (ANOVA) followed by Tukey-Kramer multiple comparisons test.

Cell cycle distribution analysis. Cells grown in 6-well plates were rinsed twice with PBS and synchronized by incubation in serum-free media with 0.5 mg/ml BSA for 36 h. H7372-31-2 was added during the last 12 h of the 36-h serum-starvation period, and the cells remained in the presence of H7372-31-2 after addition of serum to 10% of final medium volume. At

0-hour time-point (no serum addition) and different time-points after serum stimulation, cells (60-80% confluency) were harvested and fixed with 70% ethanol for overnight at -20˚C. The fixed cells were washed once with PBS/BSA, treated with 20 μg/ml RNase A (Amresco) for 30 min at 37˚C, and then stained with 40 μg/ml PI. The cells were analyzed by flow cytometry (FACSCalibur™ with CellQuest software). Approximately 15,000 cells were acquired and percentages of cells in the G0/G1, S, and G2/M phases were determined by FCS Express Version 3 software. Three independent experiments were performed.

In vitro invasion assay. Basement membrane invasion assay was done by using the invasion chamber as described previously (10) with some modifications. The microporous (8-μm pore-size) polyethylene terephthalate (PET) membrane of the cell culture insert (24-well format; BD Biosciences) was coated with undiluted basement membrane matrix (Matrigel™ , phenol red-free; BD Biosciences) following the thin gel method as described in the manufacturer's instructions. The MDA-MB-231 cells ($5x10^4$) resuspended in 200 μl of serum-free medium with 0.5 mg/ml BSA and 0.2 or 2 μg/ml H7372-31-2 were pipetted into the upper chamber. The lower chamber was filled with 700 μl of medium with similar contents but without cells. After incubation for 12 or 24 h at 37˚C, the medium at lower chamber was replaced with medium containing 10% FBS only. Following 24 h of stimulation by the chemoattractant, the culture insert was immersed in 95% ethanol for 2 min to fix the cells. After washing insert with PBS, the cells at upper surface of membrane were stained with 1 μg/ml DAPI (4',6-diamidine-2'-phenylindole; KPL, Gaithersburg, MD) for 2 min. In order to prevent non-specific DAPI staining of cells at lower surface, the lower chamber was filled with PBS until its level was higher than the level of DAPI solution in the upper chamber. The staining of cells at lower surface with 1 μg/ml PI (Sigma-Aldrich, St. Louis, MO) was done vice versa. Finally, the membrane was removed from the insert using a scalpel blade and mounted onto a glass microscope slide using fluorescent mounting media (KPL).

Entire membrane was viewed microscopically in a zig-zag pattern under magnification x200 and a total of 24 to 27 non-overlapping fields were obtained for cell quantification. Photomicrographs of DAPI and PI staining were captured individually from each field using a CCD camera (ColorView12; Olympus Soft Imaging Solutions GmbH, Münster, Germany), installed on an Olympus BX51 fluorescence microscope (Olympus, Tokyo, Japan) and attached to a computer. The photomicrographs were viewed using image-analytical software (analySIS; Olympus Soft Imaging Solutions GmbH) and evaluated for the numbers of DAPI- or PI-stained cells by counting manually with the assistance of a 'touch count' function provided by the software. The number of invaded cells (PI-stained cells) was divided by the number of non-invaded cells (DAPI-stained cells) in each field to obtain a ratio value representing the invasive capacity. The differences of mean ratio values between treated and control samples were statistically tested using Kruskal-Wallis test followed by Dunn's multiple comparisons test. To test for the reproducibility, a total of three independent experiments were performed. In each experiment, the average ratio value of a treated sample was normalized to that of corresponding control. The differences of mean normalized values of three independent experiments with control value (set to 1) were tested by one-sample t-test.

Proteolytic activity assay. The analysis of proteolytic activity in MDA-MB-231s cell was performed using the *in situ* zymography approach with quenched fluorogenic substrate (DQ™ collagen type IV, fluorescein conjugate; Invitrogen Corp.) as described previously (11) with some modifications. The DQ-collagen IV (25 μg/ml) mixed in Matrigel was used to coat the cover glasses (13-mm diameter) in 24-well plate following the thin gel method similar to that in invasion assay. The MDA-MB-231 cells ($10x10^4$) resuspended in 700 μl of serum-free medium with 0.5 mg/ml BSA and 0.2 or 2 μg/ml H7372-31-2 were pipetted into each well. After incubation for 12 or 24 h at 37˚C, serum was added to the medium at a final concentration of 10%. Following 12 h of stimulation, the cells were fixed with 95% ethanol and stained with 1 μg/ml DAPI. Photomicrographs of DAPI and FITC staining were captured individually from each field in a total of 15 non-overlapping fields (magnification x100). The numbers of DAPI-stained cells were evaluated as described in the invasion assay. Integrated density of the FITC staining of each photomicrograph was quantified by using the public domain software ImageJ [National Institutes of Health (NIH), USA]. The integrated density of fluorescence normalized with cell number in each field represents the proteolytic activity. The differences in proteolytic activity between treated and control samples were statistically tested as described in the invasion assay. Three independent experiments were performed.

Semi-quantitative Western blot analysis. MCF-7 and MDA-MB-231 cells were treated with H7372-31-2 similarly as described in the cell cycle analysis. At the end of each experiment, cells in the Petri dishes were rinsed with cold-PBS and then lysed with 1X SDS sample buffer [62.5 mM Tris-HCl (pH 6.8), 2% SDS, 10% glycerol, 100 mM DTT]. The cell lysate was homogenized by passing it through a 27-gauge needle. Each protein sample (20 μg) was electrophoresed in an SDS polyacrylamide gel and electro-transferred to a PVDF membrane. The membrane was incubated in 5% BSA blocking buffer for 1 h at room temperature. The membrane was then probed with a primary antibody for 1 h at room temperature or overnight (~18 h) at 4˚C. The primary antibodies and respective dilutions are listed in Table I. The immunoreactivity was detected by using a horseradish peroxidase-conjugated anti-rabbit or anti-mouse secondary antibody. Finally, the membrane was incubated with chemiluminescent substrate (Thermo Fisher Scientific) and visualized using the FluorChem™ 5500 imaging system (Alpha Innotech Corp., San Leandro, CA). The blot images were captured and adjusted for brightness and contrast for minimum background. Band intensities were evaluated by densitometric analysis using the ImageJ software (NIH, USA). The band intensity values of targets were normalized to those of α-tubulin obtained on the same blot to correct variations in loading and transfer among samples. Furthermore, the ratios of phosphorylated target to its total protein values were also

Table I. Primary antibodies used for Western blot analysis.

Protein	Clone	Company	Catalog no.	Antibody dilution/ incubation time
p-Rb (S807/811)	Polyclonal	Cell Signaling Technology	9308	1:1000/o.n
p-Rb (S795)	Polyclonal	Cell Signaling Technology	9301	1:1000/o.n
Rb	4H1	Cell Signaling Technology	9309	1:1000/o.n
p-CDC2 (Y15)	Polyclonal	Cell Signaling Technology	9111	1:1000/o.n
CDC2	A17.1.1	Thermo Fisher Scientific (Lab Vision), Fremont, CA	MS-110-P0	1:3000/o.n
CDK2	2B6 + 8D4	Thermo Fisher Scientific (Lab Vision)	MS-617-P0	1:1000/o.n
CDK4	DCS156	Cell Signaling Technology	2906	1:1000/o.n
CDK6	DCS83	Cell Signaling Technology	3136	1:1000/o.n
Cyclin D1	DCS6	Cell Signaling Technology	2926	1:1000/o.n
Cyclin D3	DCS22	Cell Signaling Technology	2936	1:1000/o.n
PCNA	PC10	Dako, Carpinteria, CA	M0879	1:3000/o.n
α-tubulin	DM1A	Thermo Fisher Scientific (Lab Vision)	MS-581-P	1:5000/1 h

P-, phospho-; S, serine; Y, tyrosine; o.n, overnight; Rb, retinoblastoma protein; CDC, cell division cycle; CDK, cyclin-dependent kinase; PCNA, proliferating cell nuclear antigen.

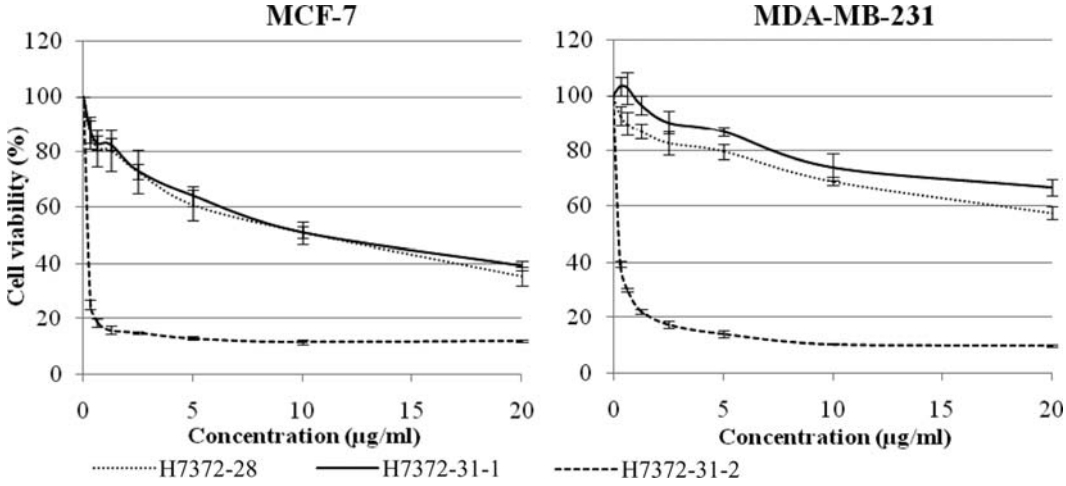

Figure 1. Dose-effect of the three active fractions, namely H7372-28, -31-1, and -31-2 on cell viability in two breast cancer cell lines after 72 h of treatment. Data represent the means ± SD of three independent experiments, each performed in triplicate.

calculated. The normalized or ratio value from each sample was divided by the value in the control at 0 hour. The data are presented as 'fold change' in comparison with that of the control at 0 hour which was set as 1. Two independent experiments were conducted.

Statistical analysis. Statistical analysis was performed using GraphPad InStat version 3.05 for Windows (GraphPad Software, Inc., San Diego, CA) as described in the apoptosis, *in vitro* invasion, and proteolytic activity assays. The data analyzed by one-sample t-test passed the normality test using the method of Kolmogorov and Smirnov. A two-sided $P<0.05$ was considered statistically significant.

Results

Effects of purified fractions on cell viability. The effects of three active fractions (H7372-28, -31-1, and -31-2) at various concentrations on cell viability were examined in two human breast cancer cell lines, MCF-7 and MDA-MB-231. Of these fractions, H7372-31-2 was revealed to be the most active as it reduced the cell viability markedly in both cancer cell lines after 72 h (Fig. 1). It was noted that the IC_{50} (concentration required to reduce cell viability to 50% of the control value) of H7372-31-2 against MCF-7 and MDA-MB-231 cells was <0.31 µg/ml unlike H7372-28 and H7372-31-1 which showed IC_{50} values of 10.43±2.4 and 10.47±1.3 µg/ml,

Table II. The IC_{50} values of 31-2 against 15 human carcinoma and 2 non-malignant cell lines in 72 h.

Cell lines	IC_{50} (μg/ml)
Nasopharyngeal carcinoma	
TW01	0.85
TW04	1.75
TW06	0.35
SUNE-1	0.5
CNE-1	2.75
Breast adenocarcinoma	
MDA-MB-231	0.45
MCF-7	0.15
T-47D	>4
Colon adenocarcinoma	
HT-29	0.35
Caco-2	0.5
HCT116	0.65
Prostate adenocarcinoma	
PC-3	0.2
DU145	0.5
Hepatocyte carcinoma	
HepG2	2.2
Cervix epitheloid carcinoma	
HeLa	0.1
Human hepatic stellate cells	
LX-2	0.65
Human fetal lung fibroblast	
IMR-90	0.3

respectively, against MCF-7 cells and IC_{50} values >20 μg/ml against MDA-MB-231 cells.

As H7372-31-2 (hereafter described as 31-2) shown to be the best performer, it was further tested against a panel of 15 human cancer and 2 non-malignant cell lines. MCF-7 and MDA-MB-231 cells were also included as a different range of 31-2 concentrations was used in this experiment. 31-2 was able to exert the growth-inhibitory effect on all the human cancer cell lines and the non-malignant IMR-90 and LX-2 cells. Table II summarizes the IC_{50} values ranging from 0.1 to 2.75 μg/ml for 31-2 against all the cell lines tested except T-47D (IC_{50} >4 μg/ml).

Effect of 31-2 on cell proliferation in MCF-7 and MDA-MB-231 cell lines. We further elucidated whether the growth inhibition observed in 31-2-treated cells was attributable to a cytotoxic or a cytostatic effect. We assessed the viability of MCF-7 and MDA-MB-231 cells every 12 h, up to 72 h, in

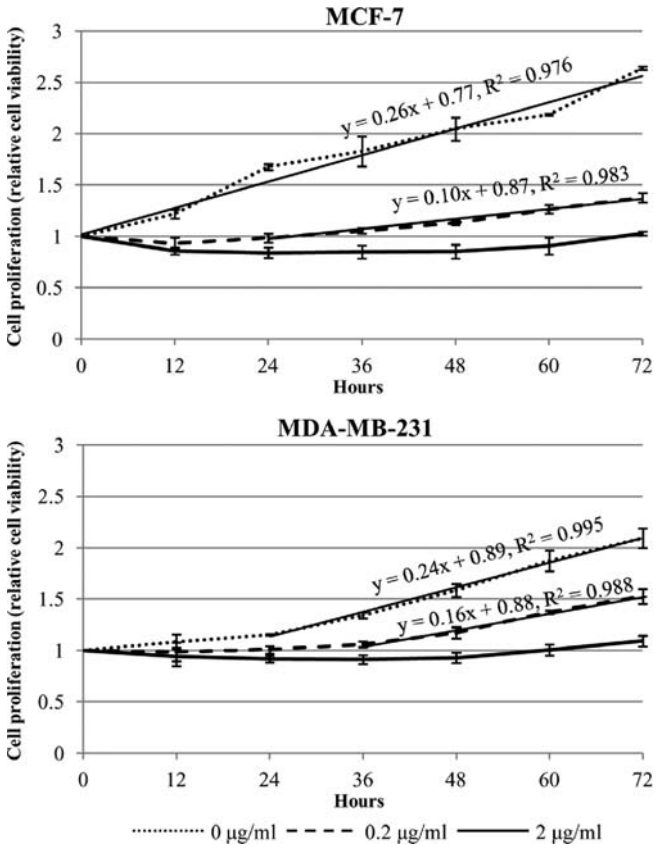

Figure 2. Kinetics of growth suppression by 31-2 in MCF-7 and MDA-MB-231 cells. Viable cell densities were assessed every 12 h, up to 72 h, by using an MTS assay and expressed as cell viability relative to hour 0 values. Data represent the means ± SD of three independent experiments, each performed in triplicate.

treatment concentrations at 2 μg/ml, which is roughly at the plateau level of their dose-effect curves, and at 10 times lower, 0.2 μg/ml. These concentrations caused approximately the highest and 50% growth inhibition, respectively, in MCF-7 and MDA-MB-231 cells (Fig. 1 and Table II).

Fig. 2 shows the kinetics of growth response to 31-2 in MCF-7 and MDA-MB-231 cells. 31-2 noticeably inhibited the proliferation of both cancer cell lines in a dose-dependent manner during 72 h of observation. 31-2 at 2 μg/ml led to complete cytostasis as evidenced by the lack of change in cell proliferation over time. Although there were slight reductions of relative cell viability seen in both cell lines treated at 2 μg/ml, this may be likely due to the normal cell death in culture rather than 31-2-triggered cell death. The proliferation rate (slope of exponential or log phase of the growth curve) of untreated MCF-7 and MDA-MB-231 cells was comparable. The relative proliferation rate of 0.2 μg/ml-treated MDA-MB-231 cells to control (0 μg/ml) cells was 1.7 times higher than that observed in MCF-7 cells, indicating the higher susceptibility of MCF-7 cells to 31-2.

Effect of 31-2 on cell apoptosis in MCF-7 and MDA-MB-231 cell lines. To further support the cytostatic effect of 31-2, its ability to induce cell apoptosis/death in MCF-7 and MDA-MB-231 cell lines was assessed using the fluorescein-

Table III. Effect of 31-2 at 0.2 and 2 μg/ml on cell apoptosis of MDA-MB-231 cells in 24, 48, and 72 h.

		% of cells		
	31-2 (μg/ml)	24 h	48 h	72 h
Early apoptotic cells	0	1.50±0.30	1.61±0.19	1.48±0.33
	0.2	2.46±1.40	0.80±0.25[a]	0.37±0.08[a]
	2	2.36±1.73	0.59±0.12[a]	1.14±0.04[d]
Late apoptotic cells	0	2.84±1.28	4.17±0.51	4.37±2.02
	0.2	2.83±1.00	2.83±0.04[a]	0.93±0.39
	2	1.99±1.14	1.75±0.13[b,c]	2.49±1.18
Necrotic cells	0	6.10±0.85	6.86±3.21	8.66±1.16
	0.2	3.35±2.03	6.36±1.61	9.33±1.15
	2	3.86±2.08	4.28±2.44	8.80±2.26

Data represent the means ± SD of three independent experiments. [a]P<0.01, [b]P<0.001 vs. 0 μg/ml (control); [c]P<0.05, [d]P<0.01 vs. 0.2 μg/ml.

labeled Annexin V/propidium iodide (Annexin V-FITC/PI) staining and flow cytometry analysis. 31-2 showed no significant induction of either apoptosis or necrosis up to 72 h of treatment in MCF-7 cells (data not shown). Similarly, no significant effect on necrosis of MDA-MB-231 cells by 31-2 was observed (Table III). However, significant reductions in early and late apoptosis were observed at 48 h of treatment and only early apoptosis at 72 h of treatment, as compared to the respective controls (Table III). In these significant reductions, the percentages of treated (0.2 and 2 μg/ml) MDA-MB-231 cells were 1.5-4 times lower than that of untreated cells. Because of the low percentages of early or late apoptosis in control cells (<4.5%), it should be noted that the differences with the treated cells are <2.5% of total cell population. Therefore, it appears that the reduction of early or late apoptosis in treated cells relative to the total cell population is not significant. The findings of regular and slightly reduced cell death in 2 μg/ml 31-2-treated MCF-7 and MDA-MB-231 cells, respectively, may also support our observation of slight decreases of relative cell viability over time in MCF-7 cells and, to a lesser extent, in MDA-MB-231 cells with similar treatment (Fig. 2). Respective cell lines treated with staurosporine were included in each staining experiment serving as positive control and in both, strong induction of early apoptosis was observed (data not shown).

Effect of 31-2 on cell cycle distribution in MCF-7 and MDA-MB-231 cell lines. In order to more clearly demonstrate the actions of 31-2 during a specific phase of the cell cycle, the MCF-7 and MDA-MB-231 cells were synchronized by switching them to serum-free media for 36 h to render them quiescent. Subsequently, 31-2 was added during the last 12 h of the 36-h serum-starvation period, and the cells remained in the presence of 31-2 after addition of serum to 10% of final medium volume. Fig. 3 shows the effect of 31-2 on the progression of synchronized MCF-7 and MDA-MB-231 cells through the cell cycle after stimulation with 10% FBS. In the absence of 31-2, serum-stimulated MCF-7 cells readily proceeded to enter the S phase at 12 hours, whereas, in its presence (0.2 and 2 μg/ml), the cells remained arrested at the G0/G1 phase. This effect was found to occur in a dose-dependent manner. In comparison with the untreated cells, MCF-7 cells treated at lower concentration (0.2 μg/ml) showed a slight and delayed decrease (at 24 hours) in percentage of cells in the G0/G1 phase due to the small progression to S phase. In contrast, at a higher concentration (2 μg/ml) of 31-2, cells exhibited a slight increase of percentage in the G0/G1 phase and then a smaller progression to S phase at more delayed time-points (at 36-60 hours) as compared to the 0.2 μg/ml-treated cells. After 24 h, 0.2 μg/ml-treated and untreated cells entered the G0/G1 phase gradually.

Unlike the observation in MCF-7 cells, untreated MDA-MB-231 cells showed no marked G1-S transition immediately after serum stimulation (Fig. 3B). The cell cycle profile of MDA-MB-231 cells with treatment at lower 31-2 concentration was similar to that of untreated cells until at hour 36, from which the percentages of treated cells were slightly higher (10-15% differences) in the G0/G1 phase and concomitantly lower in the S phase. On the other hand, a higher 31-2 concentration caused an increase of cell percentage in the S phase and a corresponding decrease of cell percentage in the G2/M phase throughout the experimental time course.

Effect of 31-2 on invasiveness of MDA-MB-231 cells. Invasion through the extracellular matrix (ECM) is a crucial step in tumour metastasis. To study the effect of 31-2 on tumour invasion, we adopted a widely used *in vitro* assay that assesses the ability of tumour cells to invade through Matrigel matrix, a reconstituted basement membrane matrix derived from the Engelbreth-Holm-Swarm mouse tumour. This assay mimics the early steps of tumour invasion *in vivo*, namely the degradation of, and migration through, basement membranes (12).

Since the MCF-7 cells are relatively non-invasive *in vitro* (13), the highly invasive MDA-MB-231 cells only were used in this assay. After 12- or 24-h treatment with 31-2 at 0.2 and 2 μg/ml in serum-free medium, the MDA-MB-231 cells

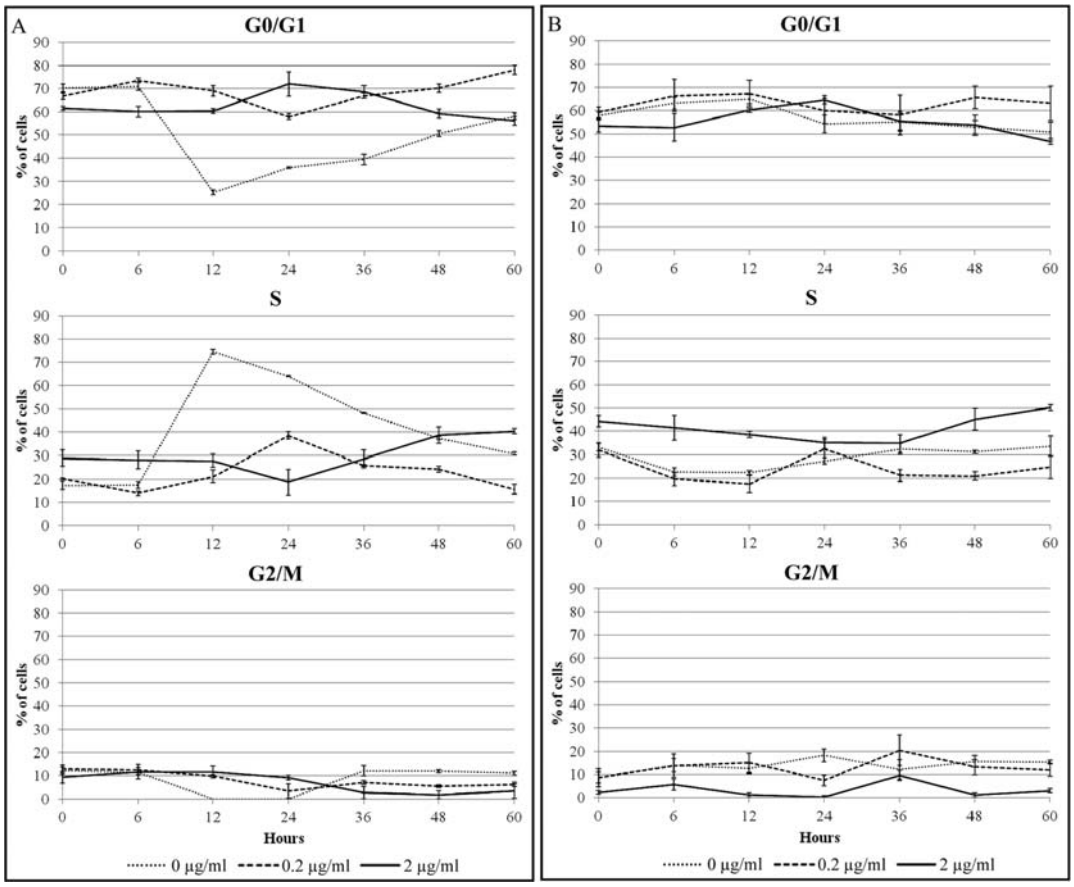

Figure 3. Effect of 31-2 on the cell cycle distribution of MCF-7 (A) and MDA-MB-231 (B) cells that were serum-starved for 36 h and then re-stimulated to enter the cell cycle by addition of 10% FBS. At various time-points after addition of serum, cells were harvested for DNA analysis by flow cytometry and the percentages of cells in the G0/G1, S, and G2/M phases of cell cycle were plotted. Data represent the means ± SD of three independent experiments.

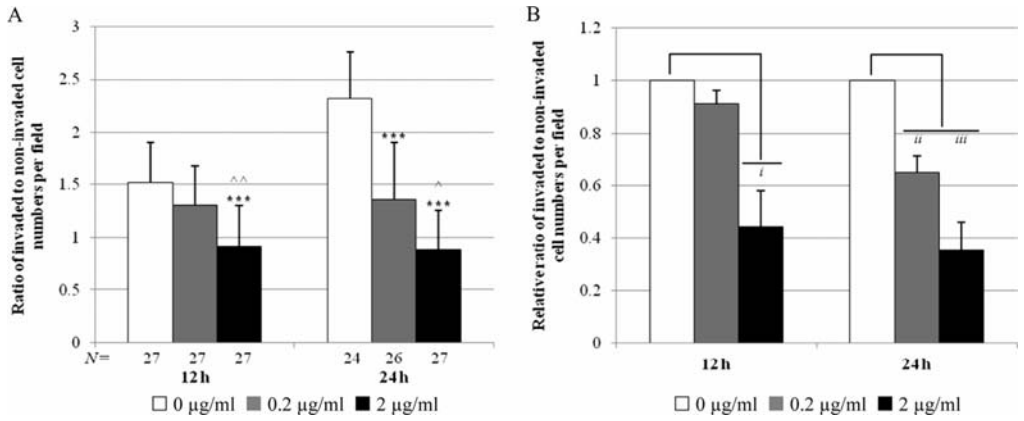

Figure 4. Inhibitory effects of 31-2 on the invasion of MDA-MB-231 cells through Matrigel after 12 and 24 h of treatment. (A) A typical experiment shows the averages ± SD of the ratios of invaded to non-invaded cell numbers calculated from 24 to 27 fields as indicated (*N*) for each membrane. Statistical analysis was done using Kruskal-Wallis test. ***P<0.001 vs. 0 µg/ml (control); ^P<0.05, ^^P<0.01 vs. 0.2 µg/ml. (B) The average ratio values in 31-2 treatments relative to that in the absence of 31-2 at respective time-points were calculated and the means ± SD for three independent experiments are shown. Statistical analysis was performed by one-sample t-test. i, P=0.02; ii, P=0.01; iii, P=0.009.

in the upper chamber (cell culture insert) were induced to invade the Matrigel, pass through the membrane pores, and emerge on the underside of the membrane by adding 10% FBS as chemoattractant to the lower chamber. In order to rule out inhibition of invasion due to the non-specific anti-proliferation effect of 31-2, the non-invaded cells were taken into account and the invasive capacity was expressed as ratio of invaded to non-invaded cell numbers, instead of counting only the number of invaded cells at lower surface of the membrane which was normally done in other evaluations (10,14,15).

The results of the invasion study are summarized in Fig. 4. The treatment of 31-2 reduced the invasive ability of MDA-MB-231 cells significantly in a dose- and time-dependent manner. In comparison with the corresponding untreated cells, the invasive ability of cells treated at 0.2 µg/ml was not altered significantly after 12 h of treatment but reduced

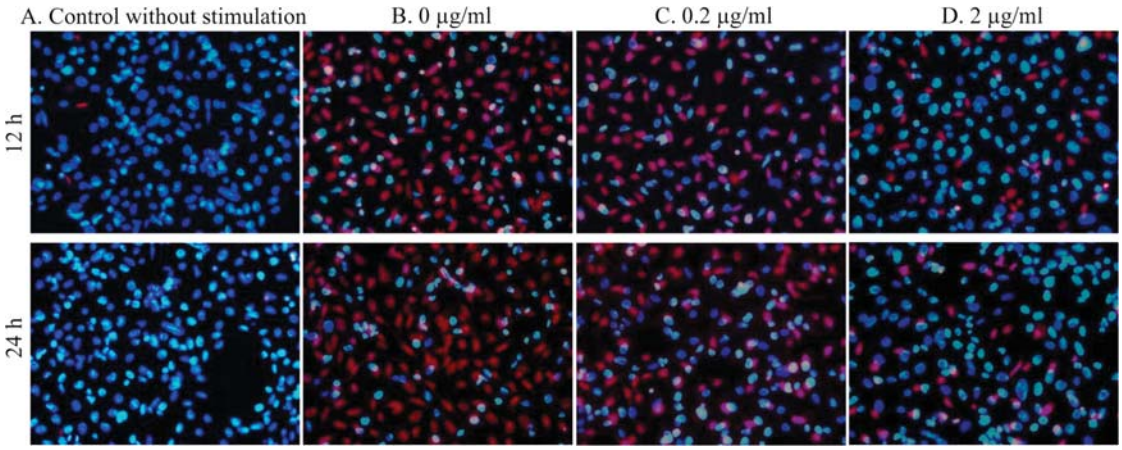

Figure 5. Each image represents the overlaid photomicrographs of upper and lower membrane surfaces captured from a similar field. After 24 h of stimulation with chemoattractant (10% FBS) (B-D) or no stimulation (A), cells invaded to the lower membrane surface were stained with propidium iodide (red) while the non-invaded cells on the upper surface of membrane were stained with DAPI (blue). Original magnification x200.

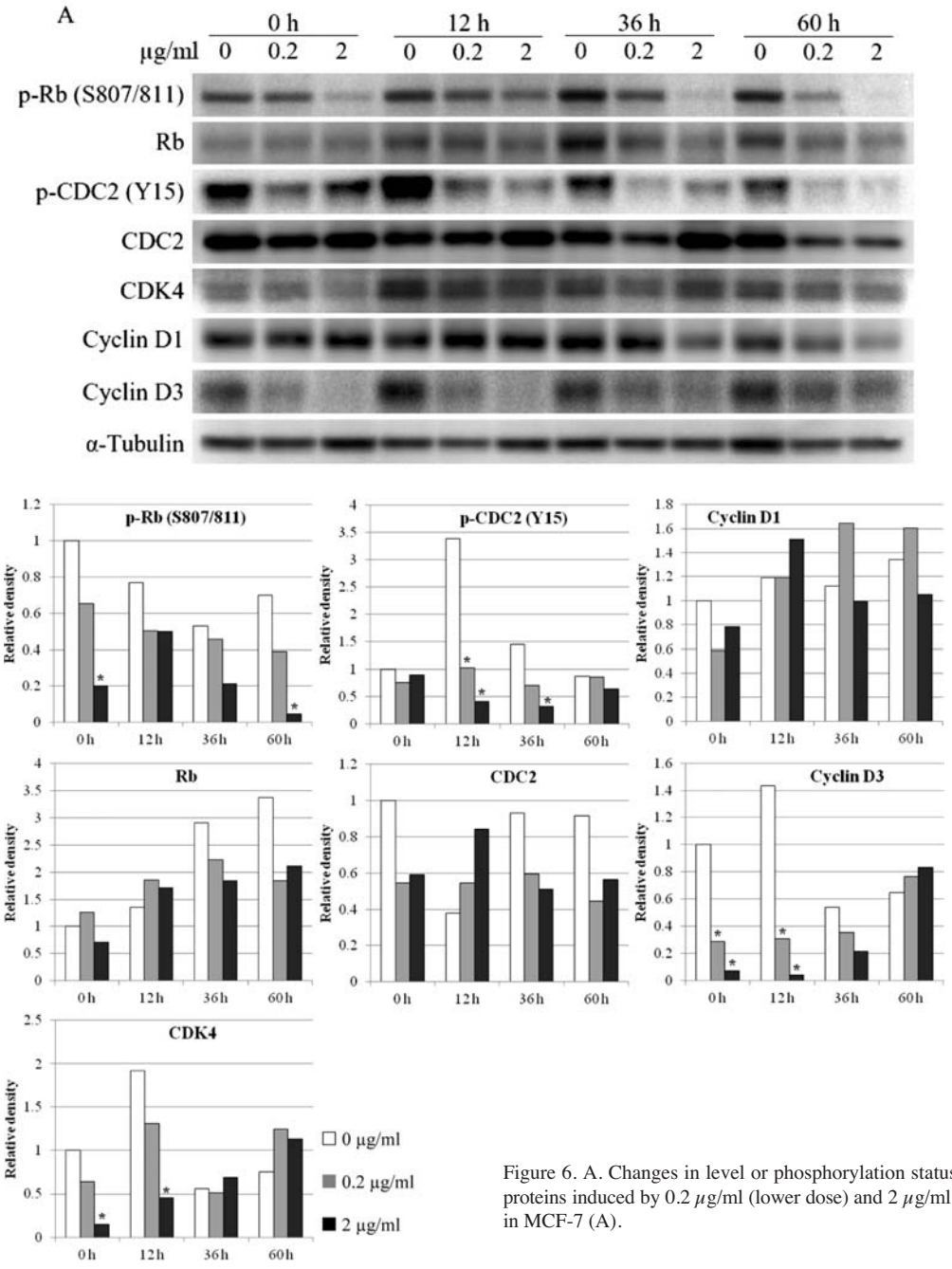

Figure 6. A. Changes in level or phosphorylation status of cell cycle-related proteins induced by 0.2 μg/ml (lower dose) and 2 μg/ml (higher dose) of 31-2 in MCF-7 (A).

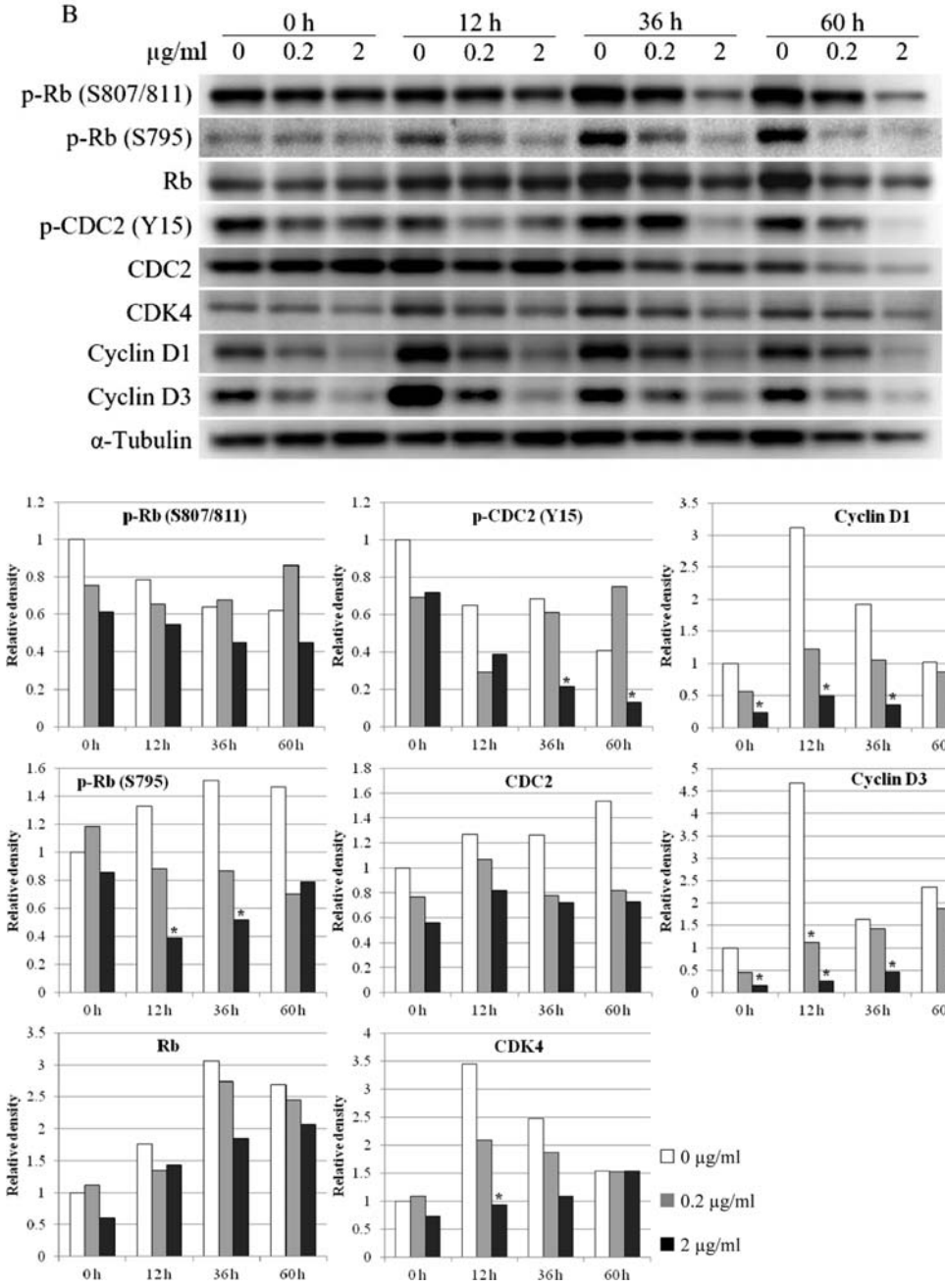

Figure 6. Changes in level or phosphorylation status of cell cycle-related proteins induced by 0.2 μg/ml (lower dose) and 2 μg/ml (higher dose) of 31-2 in MCF-7 (A) and MDA-MB-231 (B) cells. Western blotting using specific antibodies against phosphorylated (p-) and total proteins was performed and the immunoreactive bands are as shown. The band intensities were quantified by ImageJ densitometric analysis and the intensity values of targets were normalized to those of α-tubulin. In addition, the ratio of phosphorylated target to its total protein values was also calculated. Quantified results expressed relatively to control (0 μg/ml) at 0 hour are presented in the bar charts. Asterisks (*) refer to ≥3-fold differences in the relative density between treatment (0.2 or 2 μg/ml 31-2) and control (0 μg/ml) at corresponding time-points. Data are representative of one of two independent experiments with equivalent results.

significantly after 24 h of treatment (Fig. 4). The invasive capacity of cells treated at 2 μg/ml for 24 h was two to four times lower than that of the control (0 μg/ml) (Fig. 4B). The photomicrographs of representative fields in Fig. 5B-D show the inhibition of cell invasion by 31-2 treatment. There was no cell invasion in the control well without chemoattractant at the lower chamber (Fig. 5A).

Effect of 31-2 on proteolytic activity in MDA-MB-231 cells. Matrigel matrix has been shown to contain collagen IV, laminin, entactin, heparan sulfate, and proteoglycan (16). The enzymatic degradation of type IV collagen has been strongly implicated in the invasion process of various tumour cells, including breast cancer cells (17-19). To investigate whether suppression in the activity of proteases was involved in the inhibition of invasion by 31-2, the influence of 31-2 on the proteolytic activity of MDA-MB-231 cells on DQ-collagen IV, a quenched fluorescent substrate, was evaluated. After 12 or 24-h treatment with 31-2 at 0.2 and 2 μg/ml in serum-free medium, the MDA-MB-231 cells grown on the DQ-collagen IV-coated cover slip were stimulated with 10% FBS for 12 h. We found no statistically significant difference

in the cleavage of DQ-collagen IV, as indicated by the release of fluorescent peptides, after 12 or 24 h of treatment with 31-2 at 0.2 and 2 μg/ml, compared to that of no treatment (0 μg/ml) (data not shown).

Effects of 31-2 on cell cycle-related biomolecules in MCF-7 and MDA-MB-231 cells. To investigate the molecular basis of anti-proliferation exerted by 31-2 in MCF-7 and MDA-MB-231 cells, we performed semi-quantitative Western blot analysis using various antibodies including the phospho-(p-) specific antibodies to detect the expression and phosphorylation of the key biomolecules involved in the cell cycle pathways. In order to achieve the reproducibility of results obtained from two independent experiments, a 3-fold or greater difference in the expression level of a particular protein between treated and control (untreated) cells at corresponding time-points was considered to be biologically significant.

The results of Western blot analysis of cell cycle-regulated proteins in 31-2-treated MCF-7 cells are shown in Fig. 6A. Prior to serum stimulation, a higher concentration (2 μg/ml) of 31-2 significantly decreased the levels of p-Rb (S807/811), CDK4 and cyclin D3, but not cyclin D1. After serum addition, the CDK4 and cyclin D3 levels remained diminished for 12 h while the Rb phosphorylation (S807/811) was transiently elevated to the baseline level and gradually decreased to a significant level at hour 60. It was noted that the cyclin D3 level was strongly affected as a lower 31-2 concentration (0.2 μg/ml) was able to reduce its level significantly in MCF-7 cells.

In MDA-MB-231 cells, Western blot analysis (Fig. 6B) showed that the level of p-Rb (S807/811) was not affected by 31-2 treatment. However, the phosphorylation of Rb at S795, which was undetectable in treated or control MCF-7 cells throughout the experimental time course (data not shown), was decreased significantly by the higher concentration of 31-2 after 12 and 36 h of serum stimulation. In control (0 μg/ml) MDA-MB-231 cells, the serum addition resulted in a transient elevation in the levels of CDK4, cyclin D1 and cyclin D3. In contrast, the CDK4 basal level was maintained and both the expressions of cyclins D1 and D3 were diminished markedly below the baseline level in a dose-dependent manner by 31-2 throughout the treatment time course.

In addition to the expression of biomolecules that participate in regulating the G1-S progression as described above, 31-2 treatment also caused a noticeable reduction in the phosphorylation of CDC2 (also known as CDK1) on Y15, which regulates the G2-M transition, in MCF-7 (Fig. 6A) and MDA-MB-231 (Fig. 6B) cells. This effect occurred at early time-points (12 and 36 h) after serum stimulation in MCF-7 cells but at later time-points (36 and 60 h) in MDA-MB-231 cells.

The total Rb and CDC2 proteins, as well as the levels of other cell cycle-related proteins, namely CDK2, CDK6, and PCNA (data not shown), were not significantly affected by the 31-2 treatment in MCF-7 and MDA-MB-231 cells.

Discussion

In the present study, three purified fractions (H7372-28, -31-1, and -31-2) from the actinomycetes strain H7372 were shown to inhibit growth of two breast cancer cell lines tested (Fig. 1). Indeed, H7372-31-2, simplified as 31-2, exerted a much greater degree of inhibition than the other two fractions. Due to more potent growth-inhibitory effect observed in 31-2, we confined our studies to this fraction and elucidated the molecular reactions and biological responses of human cancer cells to this treatment. Our data demonstrate that 31-2 induced significant growth inhibition in various human cancer cell lines originated from different types of malignancies, including nasopharyngeal, breast, colon, hepatocellular, prostate, and cervical carcinomas (Table II). It is not surprising that two tested non-malignant human cell lines, namely hepatic stellate (LX-2) and fetal lung fibroblast (IMR-90) cells are also sensitive to 31-2 as they are continuously proliferative cell lines.

We extended our study on the 31-2 on two breast cancer cell lines representing the differentiated, non-metastatic (MCF-7) and the poorly differentiated, highly metastatic (MDA-MB-231) mammary adenocarcinomas, respectively. 31-2 was found to exert a potent anti-proliferative activity, although it failed to cause any significant loss of cell viability or apoptosis induction in both cell lines, at least during the observation period (72 h) used in this study (Fig. 2 and Table III). The 31-2-induced cytostasis suggests that cell cycle arrest was a biological response to 31-2.

Results of the cell cycle analysis indicate clearly that 31-2 induced G1 arrest in MCF-7 cells (Fig. 3A). On the other hand, it is difficult to confirm that the 31-2-treated cells were arrested in the G1 phase because no noticeable G1-S transition was shown in the control MDA-MB-231 cells upon serum addition (Fig. 3B). The inconsistency of our finding, whereby no G1-S progression occurred after release from serum deprivation condition with a previous report with MDA-MB-231 cells is not explainable at this time (20). However, we noted an S phase accumulation along with a decrease of cell population at the G2/M phase in response to the treatment. Presumably, the 31-2 treatment may also inhibit cell cycle at the G1 phase in MDA-MB-231 cells, since the S phase accumulation (35-50% of higher dose-treated cell population versus 20-35% of untreated cell population) appears not to fully explain the complete loss of cell proliferation (Fig. 2).

Control of the G1→S phase transition in the cell cycle is an important checkpoint in regulating cell proliferation. One regulator of this transition is the retinoblastoma protein (Rb) (21). Rb can bind to and inhibit the E2F family of transcription factors and the proto-oncoproteins MDM2 and c-Abl tyrosine kinase, resulting in cell growth suppression (22-24). Phosphorylation at particular Rb residues may only disrupt the binding of Rb to particular subsets of its interacting partners and therefore may result in differential regulation of downstream effector pathways (25,26). In the present study, 31-2 reduced the Rb phosphorylation at S807/811 in MCF-7 cells and this effect could be responsible for G1 arrest and growth inhibition (Fig. 6A). It has been demonstrated that phosphorylation of S807/811 blocks binding of Rb to c-Abl (25), leading to the release of c-Abl and activation of the tyrosine kinase in the nucleus of S phase cells (24). Moreover, multiple phosphorylation of S807, S811, T821, T826, and S780 also leads to the release of E2F from an inhibitory complex (26), allowing it to promote the transcription necessary for cell

cyle progression into late G1 and S phases (27). Unlike the observation in MCF-7 cells, Rb phosphorylation at S807/811 was not affected but the phosphorylation of S795 was reduced significantly by 31-2 in the MDA-MB-231 cells (Fig. 6B). Phosphorylation of S795 residue was shown to be critical for inactivation of Rb and its G1 phase arrest function (28). Further investigation showed that the phosphorylation of S795 is required for dissociation of E2F from Rb, enabling the G1-S transition (29). Based on these published data, our finding of repressed Rb phosphorylation at S795 supports the G1 phase arrest by 31-2 in MDA-MB-231 cells although this effect was not shown obviously in the cell cycle analysis (Fig. 3B).

Rb phosphorylation is catalyzed by cyclin-dependent kinases (CDKs) whose interaction with specific cyclin regulatory subunits is required for the kinase activity. There are several different cyclin-CDK combinations, including D-type cyclins in combination with CDK4 or CDK6 as well as cyclin E or cyclin A associated with CDK2. Evidence is emerging that various CDKs differentially phosphorylate Rb at distinctive residues *in vitro* and *in vivo* (28,30-32). Previous studies showed that the S807/811 residue is one of the target phosphorylation sites of CDK4 with cyclin D1 rather than cyclin D3 (31,32). Consistent with these reports, decreased CDK4 level by 31-2 in our observation is associated with reduced p-Rb (S807/811) level in MCF-7 cells at the beginning of experiment but later, this association is inconsistent (Fig. 6A). In addition, the phosphorylation of S807/811 was not affected although both cyclin D1 and CDK4 levels were decreased by 31-2 in MDA-MB-231 cells (Fig. 6B). This discrepancy might be due to other regulatory mechanisms involved in the S807/811 phosphorylation. A regulatory motif in Rb has been shown to control the exposure of the CDK sites specifically at S807/811 that determine both conformation and growth suppressing activity of Rb (33). It is possible that the regulatory motif of Rb in MDA-MB-231 cells could increase the accessibility of kinases to the CDK sites, enabling it to be phosphorylated at S807/811 readily even though in the presence of lower cyclin D1-CDK4 level. Another possibility is that the S807/811 residue might be phosphorylated more efficiently by other cyclin-CDK complexes than by cyclin D1-CDK4. Indeed, cyclin D1-CDK4 complex has been reported to phosphorylate preferentially the S795 residue and, to a much lesser degree, the S807, S811, T821 and T826 residues (34). Moreover, S795 is phosphorylated selectively by the cyclin D1-CDK4 complex, but not cyclin-CDK2 complexes (28). In correlation with these studies, we found a significant reduction of cyclin D1 and CDK4 levels accompanying decrease of Rb phosphorylation at S795 in 31-2-treated MDA-MB-231 cells (Fig. 6B). As supported by a recent study (31), the decreased S795 phosphorylation can also be attributed to the significant inhibition of cyclin D3 expression as observed in 31-2 treatment.

The level of CDK6, another kinase known to phosphorylate Rb at S807/811 and S795 with comparable efficiency to CDK4 *in vitro* (35), was unaffected by 31-2 in the present study (Fig. 6), suggesting that the repressed phosphorylation on these residues in MCF-7 and MDA-MB-231 cells, respectively, is a consequence of the decreased level of CDK4 rather than CDK6. CDK4/6 becomes active before CDK2 during the G1 phase, and studies suggest that phosphorylation of Rb by CDK4/6 may be required for its subsequent phosphorylation by CDK2 in the late G1 phase (36-38). Although we have not been able to detect any change in CDK2 level due to 31-2 treatment (Fig. 6), our data suggest that 31-2 might block inactivation/phosphorylation of Rb, at least in part, through reducing the cyclin D-CDK4 activity that prevents further hyperphosphorylation by cyclin-CDK2 complexes. PCNA is a key regulator of S phase with essential roles in DNA synthesis associated with both DNA replication and repair (39). Biochemical studies showed that PCNA binds to the cyclin-CDK complexes as well as the CDK inhibitor p21, suggesting a functional role for their interactions in cell cycle control (40). In our study, however, the levels of PCNA do not appear to be involved in the cell cycle arrest induced by 31-2 (Fig. 6).

Cell division cycle 2 (CDC2), also known as CDK1, together with its pivotal activating partner cyclin B is the key regulator of mitotic transition. In addition to the activation by cyclin B, CDC2 activity can be negatively regulated through Y15 phosphorylation by Wee1 and Myt1 tyrosine kinases during G1, S and G2 phases (41-43). This inhibitory phosphorylation is removed by CDC25 phosphatases, converting CDC2 into the active form during the G2-M transition (44). Elevated levels of CDC2 (Y15) phosphorylation are found to be associated with accumulation of the S phase (45,46). Consistent with these reports, the G1-S progression resulting in cell accumulation in the S phase was exhibited concurrently with increased p-CDC2 (Y15) level in the untreated MCF-7 cells after 12 h of serum stimulation (Figs. 3A and 6A). In the G1 arrest induced by 31-2, the p-CDC2 (Y15) levels were retained or unexpectedly, decreased by higher dose until 36 h upon serum stimulation. Similarly to MDA-MB-231 cells, there were decreases in Y15 phosphorylation of CDC2 due to 31-2 treatment even though the cell population increased in the S phase and decreased in the G2/M phase (Figs. 3B and 6B). Although dephosphorylation of CDC2 is correlated well with mitosis activation, the presence of cyclin B, which is yet to be determined here, is also required for the mitotic entry (43). A recent study demonstrated that CDC2 is inactivated during mitotic exit and interestingly, the reactivation of CDC2 by removing the inhibitory phosphorylations, together with preservation of cyclin B allows reversal to M phase even from late G1, at which may also induce cell death (43). Our finding of 31-2-repressed Y15 phosphorylation raises the possibility that 31-2 may exert inhibition of Wee1/Myt1 and/or activation of CDC25. In addition to these effects, the status of CDC2 activity and whether they are responsible for the growth-suppressive properties of 31-2 remain to be elucidated.

Basement membrane, a dynamic thin sheet-like structure of extracellular matrix, acts as a barrier separating the epithelium from the surrounding stroma and its disruption is associated with different stages of invasive carcinomas (47,48). Matrigel matrix, a basement membrane-like material produced by the mouse Engelbreth-Holm-Swarm sarcoma tumour, has been used extensively as a reconstituted basement membrane *in vitro* to investigate invasion of tumour cells. We found a potent anti-invasive property of 31-2 in highly invasive MDA-MB-231 cells, as revealed by a significant decrease in cell invasion

through Matrigel in a dose- and time-dependent manner (Fig. 4). This effect of 31-2 was not tested on MCF-7 cells because these cells are relatively not invasive. As invasion is a prominent initial step in metastasis, the anti-invasive capacity of 31-2 might have implications in increasing the survival time and decreasing morbidity of breast cancer patients.

Matrix metalloproteinases (MMPs) are up-regulated in cancer cells and other cells associated with the tumour microenvironment, and have been shown to be responsible for loss of basement membrane architecture (49,50). The major component of the basement membrane is known to be type IV collagen which is degraded effectively by MMP-2 and MMP-9 (51-53). We next examined whether the decrease in invasion was a result of decreased proteolysis of type IV collagen by observing the release of quenched fluorescence from the digested collagen IV with fluorescein conjugate. A previous study has shown that invasion of breast cancer cells correlates with the cleavage of this quenched-fluorescent substrates by endogenous proteases (19). However, there was no decrease in the cleavage of collagen IV by 31-2-treated MDA-MB-231 cells although their invasiveness was reduced. A similar finding with the same cell line was also observed in a published report (11), indicating that the inhibitory mechanisms of invasion may not always be through degradation of extracellular matrix components. Furthermore, another study showed that the inhibition of MDA-MB-231 cell invasiveness by a phenylalanine metabolite may not be due to a decrease in proteases but could be related to both the modification of cell structure and an increased expression of adhesion molecules (54). However, whether these mechanisms are involved in the modulation of cell invasion by 31-2 still needs to be defined.

Our data demonstrate that the purified fraction 31-2 from *Streptomyces* sp. H7372 induced cytostasis (anti-proliferation) but not cytotoxicity in MCF-7 and MDA-MB-231 breast cancer cells. Although the tested non-malignant cells are also sensitive to 31-2, the effect would be most likely cytostatic, rather than cytotoxic. Therefore, the *in vivo* toxicity is still unpredictable at this stage and needs further investigation. Induction of cell cycle arrest by 31-2 involved the molecular alterations, at least in part, in cell cycle-regulatory proteins including Rb, CDC2, CDK4, cyclin D1, and cyclin D3. Our results also suggest an anti-invasive property of 31-2 in MDA-MB-231 cells, implying that 31-2 might suppress metastasis *in vivo*. However, this anti-invasive effect is not attributed to the modulation of proteolytic activity in MDA-MB-231 cells. Further studies are required to elucidate whether some differences in the cellular and molecular modulations by 31-2 found between MCF-7 and MDA-MB-231 cells are due to the ER and/or PR status.

Acknowledgements

This study was supported by a research grant (02-01-04-SF0347) from the Ministry of Science, Technology and Innovation, Malaysia.

References

1. Grenon NN and Chan J: Managing toxicities associated with colorectal cancer chemotherapy and targeted therapy: a new guide for nurses. Clin J Oncol Nurs 13: 285-296, 2009.
2. Berdy J: Bioactive microbial metabolites. J Antibiot (Tokyo) 58: 1-26, 2005.
3. Olano C, Mendez C and Salas JA: Antitumor compounds from marine actinomycetes. Mar Drugs 7: 210-248, 2009.
4. Newman DJ and Cragg GM: Natural products as sources of new drugs over the last 25 years. J Nat Prod 70: 461-477, 2007.
5. Olano C, Mendez C and Salas JA: Antitumor compounds from actinomycetes: from gene clusters to new derivatives by combinatorial biosynthesis. Nat Prod Rep 26: 628-660, 2009.
6. Cheah HY: Isolation of actinomycetes from mangroves in Sabah and screening for inhibitors against eukaryotic signal transduction. Universiti Malaysia Sabah, 2003.
7. Voo CLY, Lai NS, Kibat C, *et al*: Actinomycetes and fungi isolated from Maliau Basin, Sabah and the screening for novel secondary metabolites against eukaryotic signal transduction and mycobacterium. J Trop Biol Conserv 3: 11-56, 2007.
8. Bellacosa A, Kumar CC, Di Cristofano A and Testa JR: Activation of AKT kinases in cancer: implications for therapeutic targeting. Adv Cancer Res 94: 29-86, 2005.
9. Dhillon AS, Hagan S, Rath O and Kolch W: MAP kinase signalling pathways in cancer. Oncogene 26: 3279-3290, 2007.
10. Borley AC, Hiscox S, Gee J, *et al*: Anti-oestrogens but not oestrogen deprivation promote cellular invasion in intercellular adhesion-deficient breast cancer cells. Breast Cancer Res 10: R103, 2008.
11. Koblinski JE, Kaplan-Singer BR, van Osdol SJ, *et al*: Endogenous osteonectin/SPARC/BM-40 expression inhibits MDA-MB-231 breast cancer cell metastasis. Cancer Res 65: 7370-7377, 2005.
12. Liotta LA: Tumor invasion and metastases: role of the basement membrane. Warner-Lambert Parke-Davis Award lecture. Am J Pathol 117: 339-348, 1984.
13. Ree AH, Bjornland K, Brunner N, *et al*: Regulation of tissue-degrading factors and *in vitro* invasiveness in progression of breast cancer cells. Clin Exp Metastasis 16: 205-215, 1998.
14. Zhen MC, Huang XH, Wang Q, *et al*: Green tea polyphenol epigallocatechin-3-gallate suppresses rat hepatic stellate cell invasion by inhibition of MMP-2 expression and its activation. Acta Pharmacol Sin 27: 1600-1607, 2006.
15. Kato-Stankiewicz J, Hakimi I, Zhi G, *et al*: Inhibitors of Ras/Raf-1 interaction identified by two-hybrid screening revert Ras-dependent transformation phenotypes in human cancer cells. Proc Natl Acad Sci USA 99: 14398-14403, 2002.
16. Kleinman HK, McGarvey ML, Hassell JR, *et al*: Basement membrane complexes with biological activity. Biochemistry 25: 312-318, 1986.
17. Liotta LA, Thorgeirsson UP and Garbisa S: Role of collagenases in tumor cell invasion. Cancer Metastasis Rev 1: 277-288, 1982.
18. Melchiori A, Albini A, Ray JM and Stetler-Stevenson WG: Inhibition of tumor cell invasion by a highly conserved peptide sequence from the matrix metalloproteinase enzyme prosegment. Cancer Res 52: 2353-2356, 1992.
19. Sameni M, Moin K and Sloane BF: Imaging proteolysis by living human breast cancer cells. Neoplasia 2: 496-504, 2000.
20. Botos J, Smith R III and Kochevar DT: Retinoblastoma function is a better indicator of cellular phenotype in cultured breast adenocarcinoma cells than retinoblastoma expression. Exp Biol Med 227: 354-362, 2002.
21. Weinberg RA: The retinoblastoma protein and cell cycle control. Cell 81: 323-330, 1995.
22. Chellappan SP, Hiebert S, Mudryj M, Horowitz JM and Nevins JR: The E2F transcription factor is a cellular target for the RB protein. Cell 65: 1053-1061, 1991.
23. Xiao ZX, Chen J, Levine AJ, *et al*: Interaction between the retinoblastoma protein and the oncoprotein MDM2. Nature 375: 694-698, 1995.
24. Welch PJ and Wang JY: A C-terminal protein-binding domain in the retinoblastoma protein regulates nuclear c-Abl tyrosine kinase in the cell cycle. Cell 75: 779-790, 1993.
25. Knudsen ES and Wang JY: Differential regulation of retinoblastoma protein function by specific Cdk phosphorylation sites. J Biol Chem 271: 8313-8320, 1996.
26. Knudsen ES and Wang JY: Dual mechanisms for the inhibition of E2F binding to RB by cyclin-dependent kinase-mediated RB phosphorylation. Mol Cell Biol 17: 5771-5783, 1997.
27. Dyson N: The regulation of E2F by pRB-family proteins. Genes Dev 12: 2245-2262, 1998.
28. Connell-Crowley L, Harper JW and Goodrich DW: Cyclin D1/Cdk4 regulates retinoblastoma protein-mediated cell cycle arrest by site-specific phosphorylation. Mol Biol Cell 8: 287-301, 1997.

29. Rubin SM, Gall AL, Zheng N and Pavletich NP: Structure of the Rb C-terminal domain bound to E2F1-DP1: a mechanism for phosphorylation-induced E2F release. Cell 123: 1093-1106, 2005.
30. Adams PD: Regulation of the retinoblastoma tumor suppressor protein by cyclin/cdks. Biochim Biophys Acta 1471: M123-M133, 2001.
31. Paternot S, Arsenijevic T, Coulonval K, Bockstaele L, Dumont JE and Roger PP: Distinct specificities of pRb phosphorylation by CDK4 activated by cyclin D1 or cyclin D3: differential involvement in the distinct mitogenic modes of thyroid epithelial cells. Cell Cycle 5: 61-70, 2006.
32. Zarkowska T and Mittnacht S: Differential phosphorylation of the retinoblastoma protein by G1/S cyclin-dependent kinases. J Biol Chem 272: 12738-12746, 1997.
33. Driscoll B, T'Ang A, Hu YH, *et al*: Discovery of a regulatory motif that controls the exposure of specific upstream cyclin-dependent kinase sites that determine both conformation and growth suppressing activity of pRb. J Biol Chem 274: 9463-9471, 1999.
34. Pan W, Sun T, Hoess R and Grafstrom R: Defining the minimal portion of the retinoblastoma protein that serves as an efficient substrate for cdk4 kinase/cyclin D1 complex. Carcinogenesis 19: 765-769, 1998.
35. Takaki T, Fukasawa K, Suzuki-Takahashi I, *et al*: Preferences for phosphorylation sites in the retinoblastoma protein of D-type cyclin-dependent kinases, Cdk4 and Cdk6, *in vitro*. J Biochem 137: 381-386, 2005.
36. Harbour JW, Luo RX, Dei Santi A, Postigo AA and Dean DC: Cdk phosphorylation triggers sequential intramolecular interactions that progressively block Rb functions as cells move through G1. Cell 98: 859-869, 1999.
37. Lundberg AS and Weinberg RA: Functional inactivation of the retinoblastoma protein requires sequential modification by at least two distinct cyclin-cdk complexes. Mol Cell Biol 18: 753-761, 1998.
38. Ezhevsky SA, Ho A, Becker-Hapak M, Davis PK and Dowdy SF: Differential regulation of retinoblastoma tumor suppressor protein by G(1) cyclin-dependent kinase complexes *in vivo*. Mol Cell Biol 21: 4773-4784, 2001.
39. Moldovan GL, Pfander B and Jentsch S: PCNA, the maestro of the replication fork. Cell 129: 665-679, 2007.
40. Maga G and Hubscher U: Proliferating cell nuclear antigen (PCNA): a dancer with many partners. J Cell Sci 116: 3051-3060, 2003.
41. Mueller PR, Coleman TR, Kumagai A and Dunphy WG: Myt1: a membrane-associated inhibitory kinase that phosphorylates Cdc2 on both threonine-14 and tyrosine-15. Science 270: 86-90, 1995.
42. Parker LL and Piwnica-Worms H: Inactivation of the p34cdc2-cyclin B complex by the human WEE1 tyrosine kinase. Science 257: 1955-1957, 1992.
43. Potapova TA, Daum JR, Byrd KS and Gorbsky GJ: Fine tuning the cell cycle: activation of the Cdk1 inhibitory phosphorylation pathway during mitotic exit. Mol Biol Cell 20: 1737-1748, 2009.
44. O'Farrell PH: Triggering the all-or-nothing switch into mitosis. Trends Cell Biol 11: 512-519, 2001.
45. Miyachi T, Adachi M, Hinoda Y and Imai K: Butyrate augments interferon-alpha-induced S phase accumulation and persistent tyrosine phosphorylation of cdc2 in K562 cells. Br J Cancer 79: 1018-1024, 1999.
46. Tyagi A, Singh RP, Agarwal C, Siriwardana S, Sclafani RA and Agarwal R: Resveratrol causes Cdc2-tyr15 phosphorylation via ATM/ATR-Chk1/2-Cdc25C pathway as a central mechanism for S phase arrest in human ovarian carcinoma Ovcar-3 cells. Carcinogenesis 26: 1978-1987, 2005.
47. Barsky SH, Siegal GP, Jannotta F and Liotta LA: Loss of basement membrane components by invasive tumors but not by their benign counterparts. Lab Invest 49: 140-147, 1983.
48. Havenith MG, Arends JW, Simon R, Volovics A, Wiggers T and Bosman FT: Type IV collagen immunoreactivity in colorectal cancer. Prognostic value of basement membrane deposition. Cancer 62: 2207-2211, 1988.
49. Overall CM and Kleifeld O: Tumour microenvironment - opinion: validating matrix metalloproteinases as drug targets and anti-targets for cancer therapy. Nat Rev Cancer 6: 227-239, 2006.
50. Vizoso FJ, Gonzalez LO, Corte MD, *et al*: Study of matrix metalloproteinases and their inhibitors in breast cancer. Br J Cancer 96: 903-911, 2007.
51. Kalluri R: Basement membranes: structure, assembly and role in tumour angiogenesis. Nat Rev Cancer 3: 422-433, 2003.
52. Jones JL and Walker RA: Control of matrix metalloproteinase activity in cancer. J Pathol 183: 377-379, 1997.
53. Zeng ZS, Cohen AM and Guillem JG: Loss of basement membrane type IV collagen is associated with increased expression of metalloproteinases 2 and 9 (MMP-2 and MMP-9) during human colorectal tumorigenesis. Carcinogenesis 20: 749-755, 1999.
54. Vasse M, Thibout D, Paysant J, Legrand E, Soria C and Crepin M: Decrease of breast cancer cell invasiveness by sodium phenylacetate (NaPa) is associated with an increased expression of adhesive molecules. Br J Cancer 84: 802-807, 2001.